

Optimized Reverse Micelle Surfactant System for High-Resolution NMR Spectroscopy of Encapsulated Proteins and Nucleic Acids Dissolved in Low Viscosity Fluids

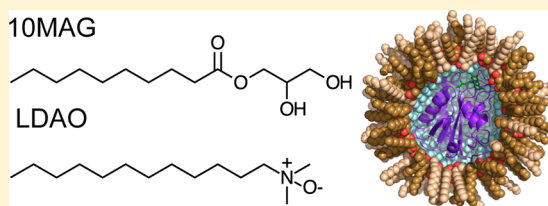
Igor Dodevski,[†] Nathaniel V. Nucci,[†] Kathleen G. Valentine,[†] Gurnimrat K. Sidhu,[†] Evan S. O'Brien,[†] Arthur Pardi,[‡] and A. Joshua Wand^{*,†}

[†]Johnson Research Foundation and Department of Biochemistry and Biophysics, University of Pennsylvania, Philadelphia, Pennsylvania 19104-6059

[‡]Department of Chemistry and Biochemistry, University of Colorado, Boulder, Colorado 80309-0596

S Supporting Information

ABSTRACT: An optimized reverse micelle surfactant system has been developed for solution nuclear magnetic resonance studies of encapsulated proteins and nucleic acids dissolved in low viscosity fluids. Comprising the nonionic 1-decanoyl-*rac*-glycerol and the zwitterionic lauryldimethylamine-*N*-oxide (10MAG/LDAO), this mixture is shown to efficiently encapsulate a diverse set of proteins and nucleic acids. Chemical shift analyses of these systems show that high structural fidelity is achieved upon encapsulation. The 10MAG/LDAO surfactant system reduces the molecular reorientation time for encapsulated macromolecules larger than ~20 kDa leading to improved overall NMR performance. The 10MAG/LDAO system can also be used for solution NMR studies of lipid-modified proteins. New and efficient strategies for optimization of encapsulation conditions are described. 10MAG/LDAO performs well in both the low viscosity pentane and ultralow viscosity liquid ethane and therefore will serve as a general surfactant system for initiating solution NMR studies of proteins and nucleic acids.



INTRODUCTION

Solution nuclear magnetic resonance (NMR) spectroscopy is a powerful technique for studying the structures of macromolecules under a variety of conditions and their internal dynamics on a wide range of time scales.¹ Sample preparation is often a key factor in being able to obtain high-quality NMR data on complex macromolecular systems. Methods for encapsulating proteins within the aqueous core of a reverse micelle, and then dissolving the micelle in low viscosity fluid, were introduced in the late 1990s to help overcome the “slow tumbling” problem presented by large, soluble proteins (Figure 1).² Since then, reverse micelles have been used to study integral^{3,4} and anchored⁵ membrane proteins, as well as soluble proteins⁶ and nucleic acids⁷ of marginal stability. Encapsulation has also enabled studies of various biophysical properties of protein including cold denaturation,^{8,9} hydration^{10,11} and internal motion.¹²

A critical issue when using reverse micelle techniques in NMR studies is that the surfactants must be able to efficiently encapsulate the macromolecule with high structural fidelity while also allowing the use of low viscosity solvents such as liquid pentane, propane or ethane. Thus, the overall size of the surfactant and the electrostatic characteristics of the headgroup are critical for maintaining the native structure while also providing the desired reduction in molecular reorientation time for the encapsulated macromolecule. Several studies have identified reverse micelle surfactant systems that meet the strict

requirements of high-resolution reverse micelle NMR,^{13,14} but a surfactant system of general utility has not yet been described. Currently, the two commonly used surfactants in reverse micelle NMR are the anionic bis(2-ethylhexyl)-sulfosuccinate (AOT)² and the cationic hexadecyltrimethylammonium bromide (CTAB),¹⁵ where the latter uses hexanol as a cosurfactant (Figure 1). Applications of AOT in this context are limited because few proteins have been encapsulated with high structural fidelity, presumably due to the denaturing effect of the anionic headgroup. CTAB has proven more successful—possibly due to the help of the nonionic cosurfactant hexanol—and has been used to encapsulate various proteins with high structural fidelity and high quality NMR spectra.^{15,16} Nevertheless, the search for optimal encapsulation conditions for a given protein has been somewhat *ad hoc*, which has likely limited general application of this approach. Thus, there is a need for a highly robust reverse micelle surfactant system that allows for efficient discovery of encapsulation conditions for a given macromolecule with high structural fidelity. Here, we describe the development of a novel surfactant system that can be generally applied to proteins and nucleic acids thus allowing for high-resolution NMR studies of a wide-range of encapsulated biological macromolecules. The experimental requirements imposed by reverse micelle NMR spectroscopy

Received: October 20, 2013

Published: February 4, 2014

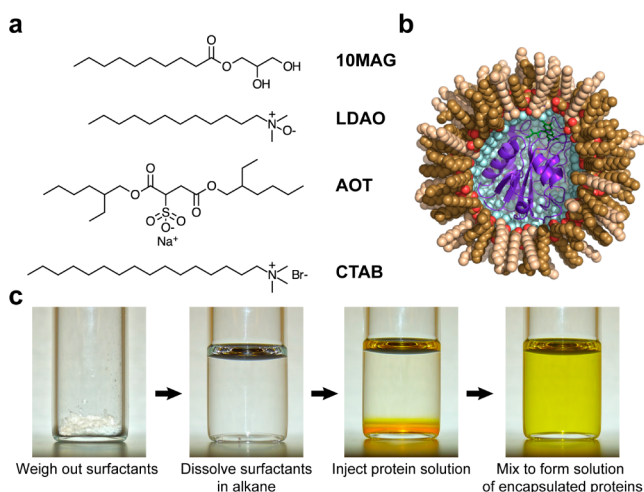


Figure 1. 10MAG/LDAO reverse micelle surfactant system for solution NMR studies of encapsulated proteins and nucleic acids. (a) Chemical structures of the nonionic/zwitterionic surfactant system 10MAG/LDAO compared to the currently used ionic surfactants AOT or CTAB. (b) Cut-away view of a space-filling model of flavodoxin encapsulated in a 10MAG/LDAO reverse micelle. (c) The direct injection method for sample preparation is illustrated using flavodoxin bound to its brightly yellow cofactor flavin mononucleotide. Conditions: 300 μ M flavodoxin in 150 mM 10MAG/LDAO surfactant at a molar percent ratio of 65%:35%, 15 mM hexanol and water loading (W_0) of 20.

led to identification of a binary surfactant system consisting of the nonionic 1-decanoyl-*rac*-glycerol (10MAG) and the zwitterionic lauryldimethylamine-*N*-oxide (LDAO). By combining a zwitterionic headgroup with a relatively short contour length tail, the 10MAG/LDAO surfactant systems provides both high biocompatibility and fast molecular tumbling for the encapsulated macromolecule.

The performance of 10MAG/LDAO was evaluated by comparing the NMR properties of a variety of reverse micelle encapsulated biological macromolecules with their properties in free aqueous solution. It is also demonstrated that 10MAG/LDAO reverse micelles provide an excellent membrane mimetic for studying lipid-modified, membrane associated proteins by solution NMR. An improved procedure that greatly simplifies sample preparation by avoiding the high protein concentrations previously required for preparing reverse micelle samples is also presented.

EXPERIMENTAL SECTION

Proteins and tRNA were isotopically labeled and purified as described in the Supporting Information (SI). All proteins and tRNA used in this study were expressed without deuteration.

Surfactant Screening. Mixtures of up to four different surfactants featuring nonionic, ionic, or zwitterionic head groups and different types of linear, branched, or cyclic hydrophobic tails were screened for their ability to form stable reverse micelle solutions in the absence of protein. The surfactants examined are listed in SI Table S1. Hexanol, which is typically present as a stabilizing cosurfactant in reverse micelle preparations, was not included in this initial screen. The total concentration of surfactants was kept constant at 75 mM. Solutions were prepared in hexane. The buffer for testing empty reverse micelle formation was 20 mM sodium phosphate (pH 7.0) with 50 mM NaCl. Bromophenol blue (0.2 mg/mL) was added to the buffer as a visual aid to detect reverse micelle formation. The molar ratio of water to surfactant, also known as the water loading or W_0 , was typically tested from 10 to 30. Positive surfactant combinations were defined as those

showing a single clear blue phase and the absence of any precipitate with a W_0 of at least 20. Further details may be found in the SI.

Preparation of Encapsulated Proteins and tRNA. The 10MAG/LDAO surfactants were used in a molar percent ratio of 65%:35% and at a total surfactant concentration of 75–150 mM as noted. The concentration of the cosurfactant hexanol depended on the total 10MAG/LDAO surfactant concentration and on the type of bulk alkane solvent used (pentane or ethane). Pentane samples were prepared with 10–20 mM hexanol at 75 mM surfactant and 20–30 mM hexanol at 150 mM surfactant. Ethane samples were typically prepared with 30–50 mM hexanol at 75 mM surfactant and 60–70 mM hexanol at 150 mM surfactant. Further details may be found in the SI.

Reverse micelle samples in liquid ethane were prepared using specialized apparatus from Daedalus Innovations, LLC (Aston, PA). LDAO, 10MAG, and hexanol were dissolved in 300 μ L of d_{12} -pentane and transferred to the mixing chamber (1.65 mL nominal volume) of a Daedalus Innovations RM Synthesizer unit. A volume of concentrated protein solution yielding the desired final W_0 was added and the mixing chamber was sealed. Pressurized liquid ethane was pumped into the mixing chamber with an Isco 65D (Lincoln, NE) syringe pump while the sample was being stirred. The sample pressure was increased until a distinct phase transition from a cloudy suspension to a clear solution was observed. This generally occurred in the range of 275–450 bar though higher pressures were sometimes required for macromolecules of larger size and/or at higher concentrations. After completion of mixing, the sample pressure was adjusted to 14–20 bar above the observed encapsulation (transition) pressure. The sample was then transferred¹⁷ to a high-pressure 3.6 mm i.d. NMR cell rated to 1 kbar (Daedalus Innovations, LLC, Aston, PA) for further analysis by NMR. The final sample contained 80% (v/v) ethane and 20% (v/v) pentane.

For samples prepared by the injection–evaporation method, water, alkane solvent, and to some degree volatile surfactants such as hexanol are removed under a gentle stream of N_2 gas. The pentane solvent and volatile components other than water are replenished, as indicated by 1H NMR spectra, to rebalance the surfactant mixture. Another round of injection can then take place. Each round takes \sim 5 min. By repeating these steps the amount of encapsulated macromolecule accumulates in the sample. See Supporting Information for further details.

NMR Spectroscopy. NMR spectra were obtained using Bruker Avance III NMR spectrometers equipped with 5 mm cryogenically cooled triple resonance probes. Samples were locked on the deuterated alkane solvent. All data were collected at 25 $^{\circ}C$. Standard two- and three-dimensional heteronuclear NMR pulse sequences were used to assess spectral perturbations.¹ Effective molecular reorientation correlation times ($\tilde{\tau}_m$) were estimated using the ^{15}N -TROSY-based (TRACT) relaxation experiment.¹⁸ To determine $\tilde{\tau}_m$, multiple portions of the amide (or imino) region were integrated and that which gave the highest measured $\tilde{\tau}_m$ is reported. Error was estimated from the variance in integrated area for duplicate relaxation delay points. This error was far smaller than that imposed by the rigid body approximation assumed in the TRACT analysis. In order to more rigorously compare the tumbling of encapsulated MBP to that in aqueous solution, ^{15}N T_1 , T_2 and heteronuclear NOE experiments¹⁹ were collected at 750 and 600 MHz. For comparison of ^{15}N T_2 values, T_2 relaxation of aqueous MBP was collected at 750 MHz using a TROSY-based pulse sequence.²⁰ T_1 and T_2 experiments were collected using six delay times with two collected in duplicate for error analysis. Rotational correlation times were determined by fit to an isotropic tumbling model using in-house software.²¹ Spectra were processed using Felix (Accelrys, San Diego, CA) or in-house NMR processing software (AL NMR).²² The SPARKY software package was used for spectral analysis and plotting (Goddard, T.D. and Kneller, D.G. SPARKY 3, University of California, San Francisco).

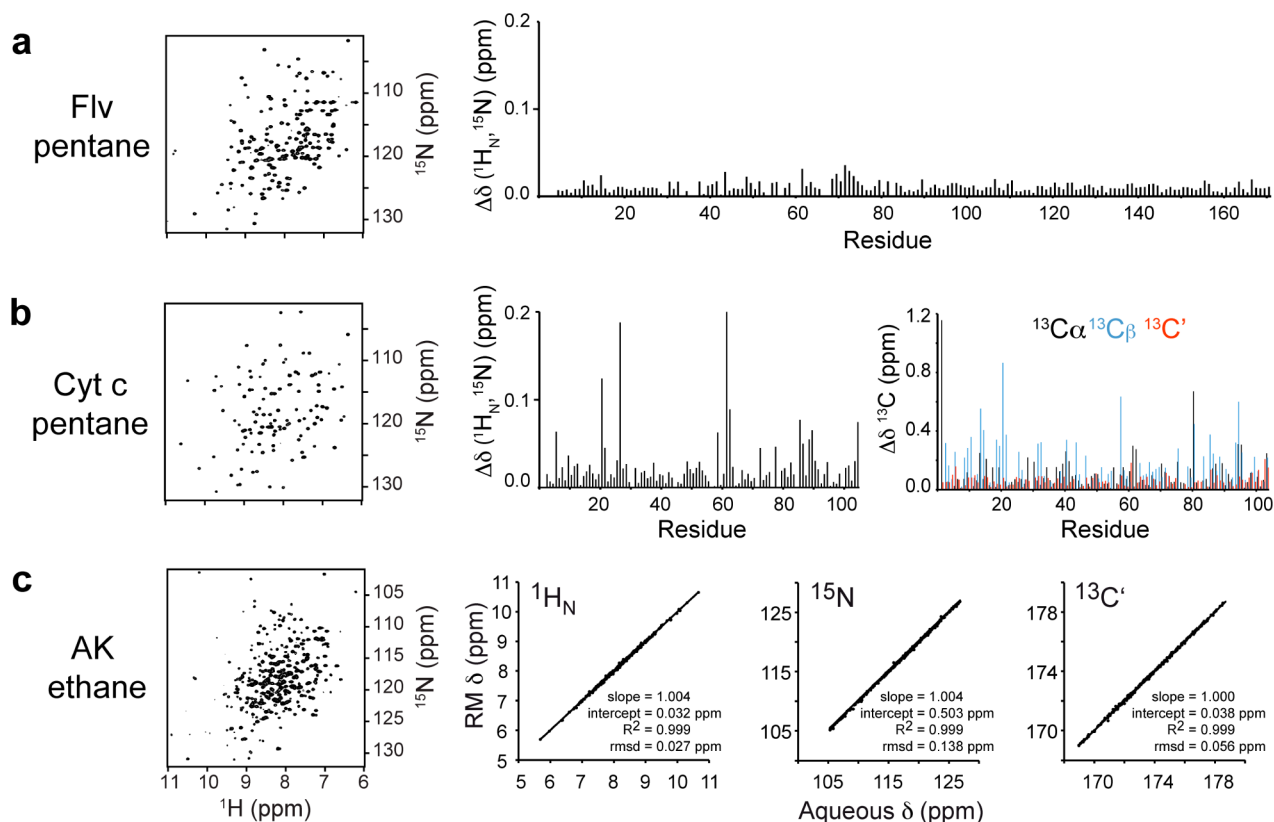


Figure 2. Encapsulation of diverse proteins with high-structural fidelity in the 10MAG/LDAO surfactant system. Proteins of distinctly different net surface charges and molecular weights retain their bulk solution structure as evidenced by minimal chemical shift (δ) perturbations upon encapsulation. (a) ^{15}N HSQC spectrum (left) of encapsulated ^{15}N -flavodoxin (18.8 kDa, $p\text{I} \approx 4.5$) in pentane acquired at 500 MHz (^1H). Histogram of gyromagnetic ratio weighted ^1H and ^{15}N chemical shift differences relative to flavodoxin in free aqueous solution²³ (right). (b) ^{15}N HSQC spectrum (left) of encapsulated horse $^{13}\text{C}, ^{15}\text{N}$ -cytochrome *c* (12 kDa, $p\text{I} \approx 11$) in pentane acquired at 600 MHz (^1H). Histograms of weighted ^1H and ^{15}N (middle) and $^{13}\text{C}_\alpha$, $^{13}\text{C}_\beta$, and $^{13}\text{C}'$ (right) chemical shift differences relative to the protein in free aqueous solution.^{24,25} (c) ^{15}N HSQC spectrum (left) of encapsulated $^{13}\text{C}, ^{15}\text{N}$ -arginine kinase (AK) (40.2 kDa, $p\text{I} \approx 6.3$) in ethane acquired at 750 MHz (^1H). Correlation of amide ^1H and ^{15}N and carbonyl $^{13}\text{C}'$ chemical shifts for AK. Encapsulated Cyt *c* and Flv were dissolved in pentane, and AK was dissolved in ethane at 380 bar. All spectra were recorded at 25 °C.

RESULTS AND DISCUSSION

Identification and Optimization of the 10MAG/LDAO Surfactant System. A systematic screen was undertaken to identify promising surfactant mixtures for reverse micelle NMR, where various mixtures were tested for their ability to form stable “empty” reverse micelles, as described in Materials and Methods and the SI. The screen consisted of mixtures of up to four different commercially available surfactants featuring nonionic, ionic, or zwitterionic headgroups and different types of linear, branched, or cyclic hydrophobic tails (SI Table S1). This screen identified a binary surfactant mixture of 1-decanoyl-*rac*-glycerol and lauryldimethylamine-*N*-oxide (10MAG/LDAO) as having highly desirable properties for encapsulation of proteins (SI Figure S1 and Table S2).

The chemical structures of 10MAG and LDAO are given in Figure 1a. The nonionic monoacylglycerol head groups of 10MAG were expected to suppress denaturing ionic interactions between the surfactant shell and the surface of an encapsulated macromolecule (Figure 1b). The zwitterionic character of LDAO was also anticipated to be similarly gentle. These properties suggested that 10MAG/LDAO should faithfully encapsulate target macromolecules independent of their net surface charge. In addition, the relatively short linear hydrophobic tails of 10MAG and LDAO (10 and 12 carbons, respectively) were anticipated to favor fast molecular

reorientation of the reverse micelle particle and thus to enhance their performance in NMR spectroscopy.

In a secondary screen we fine-tuned the molar ratio of the components of the 10MAG/LDAO reverse micelle system for optimal NMR performance. The molar ratio of water to surfactant is particularly important because larger proteins require larger encapsulation volumes to form a stable reverse micelle. Nevertheless, the total amount of water should be limited to minimize the size and achieve the fastest reorientation of the reverse micelle particle. Optimization of both the 10MAG/LDAO molar ratio and the amount of hexanol was required to achieve the desired range of water loading (W_0) (Supplementary Figure 2). The hexanol cosurfactant acts as a stabilizer of reverse micelle preparations.¹⁵ A molar ratio of 65%:35% of 10MAG:LDAO at a total surfactant concentration of 75 – 150 mM accommodated water loadings from 5 to 40, which is sufficient to fully hydrate proteins up to ~ 100 kDa. The required hexanol concentration ranged from 0 to 100 mM depending on W_0 and the alkane solvent employed. These globally optimized conditions were then used for all subsequent encapsulation studies.

Diverse proteins retain structural integrity when encapsulated in 10MAG/LDAO. A total of seven globular, water-soluble proteins were tested to determine the general utility of the 10MAG/LDAO surfactant system for reverse

micelle NMR. All seven of these proteins were successfully encapsulated in 10MAG/LDAO mixtures in pentane with minimal optimization required. W_0 and the total surfactant and hexanol concentrations were optimized to maximize encapsulation efficiency (highest encapsulated protein concentration). The seven tested proteins range from 8.5 to 81 kDa and have isoelectric points between 4.5 and 11. Five of these proteins, ubiquitin (Ub, 8.5 kDa, $pI \approx 6.8$), cytochrome *c* (Cyt *c*, 11.7 kDa, $pI \approx 11$), flavodoxin (Flv, 18.8 kDa, $pI \approx 4.5$), maltose binding protein (MBP, 40.8 kDa, $pI \approx 5.2$), and malate synthase G from *E. coli* (MSG, 81.4 kDa, $pI \approx 5.9$) have been previously encapsulated using the ionic surfactants AOT or CTAB, or a triple surfactant mixture also containing tetraethylene glycerol monododecyl ether (C12E4).^{2,13,15,16} In addition, two proteins were examined that are large by routine solution NMR standards and have not previously been studied by reverse micelle NMR: arginine kinase from the horseshoe crab *L. polyphemus* (AK, 40.2 kDa, $pI \approx 6.3$) and human aldoketo reductase 1C2 (AKR, also known as type III 3 α -hydroxysteroid dehydrogenase, 36.7 kDa, $pI \approx 7.1$).

Reverse micelle samples were prepared by the *direct injection* method,²⁶ where a specific volume of concentrated aqueous solution of protein is directly pipetted to an alkane solution of surfactants and mixed by vortexing (Figure 1c). Ub, Cyt *c*, and Flv were used to examine how the charge of the protein affects the efficiency of encapsulation. The pH of the reverse micelle water core was adjusted so that the net charge of the encapsulated protein was negative for Flv and positive for Ub and Cyt *c*. Setting the pH of the aqueous core of reverse micelles is critically important for achieving optimal encapsulation. The pH of the water core is dominated by the surfactants and only marginally influenced by the buffer employed since there are a hundred or more zwitterionic head groups and only a handful of buffer molecules per reverse micelle. Methods for adjusting the effective pH inside the water core of a reverse micelle sample have been described elsewhere.²⁷ All three proteins were encapsulated in pentane at final concentrations of 200 μ M with $W_0 = 10$ (Ub, Cyt *c*) and $W_0 = 12$ (Flv). All reverse micelle solutions were clear, showed no visible precipitate, and gave excellent ¹⁵N HSQC spectra (SI Figure S3). These samples were stable at room temperature for at least 2 months.

Comparison of the backbone chemical shifts for the protein in aqueous solution and encapsulated in the reverse micelle was used as a quantitative measure of structural integrity. For flavodoxin there are negligible differences between the amide ¹H and ¹⁵N chemical shifts in aqueous solution and encapsulated in 10MAG/LDAO (histogram in Figure 2a). A more extensive backbone chemical shift analysis (¹H_N, ¹³C α , ¹³C β , ¹³C', ¹⁵N) showed that reduced cytochrome *c* is encapsulated in 10MAG/LDAO with little apparent structural perturbation (Figure 2b). Three proteins—AKR bound to NADP⁺, MBP bound to maltose, and apo-AK—were used to assess the ability of 10MAG/LDAO to encapsulate larger proteins. Comparison of the resolved cross peaks of the ¹⁵N HSQC spectra obtained in pentane and in aqueous solution indicates that the three proteins were encapsulated in their native state (SI Figure S4). AK was more extensively examined using triple resonance spectroscopy of a sample prepared in ethane, which afforded better relaxation properties and narrower lines. An excellent chemical shift correspondence was found, demonstrating the high structural fidelity of the encapsulated protein (Figure 2c). Finally, MSG (81 kDa) was

used with minimal optimization required to demonstrate the application of the 10MAG/LDAO mixture to even larger proteins. The successful encapsulation of seven globular proteins of diverse physical characteristics with only minimal specific optimization demonstrates that 10MAG/LDAO represents a major step forward in the general applicability of the reverse micelle encapsulation methodology.

Lowering the Molecular Reorientation Time. A central advantage of the reverse micelle encapsulation strategy is the ability to manipulate the NMR relaxation properties of the macromolecule by actively decreasing the molecular reorientation time (τ_m) through the use of low viscosity solvents. Though *n*-pentane is often initially employed to explore sample conditions for encapsulation, the “volume penalty” imposed by the reverse micelle particle (water core plus surfactant shell) often outweighs gains in tumbling. Lower viscosity liquid alkanes require preparation under pressure. Reverse micelle solutions prepared with liquid butane or propane are often sufficient to overcome this “volume penalty,” thereby providing shorter molecular reorientation times for large proteins.² However, the minimum molecular reorientation time is achieved using liquid ethane.²⁸ Although only moderate pressure is required to liquefy ethane at room temperature (47 bar), considerably higher pressures are needed to support homogeneous and stable NMR samples of encapsulated proteins in condensed gases (typically 250–500 bar).^{28–34} A specialized mixing apparatus is therefore employed.¹⁷ The “volume penalty” is evident for small proteins even when encapsulated in the ultralow viscosity ethane, as shown by the higher τ_m values for encapsulated ubiquitin, cytochrome *c*, and flavodoxin shown in Figure 3.

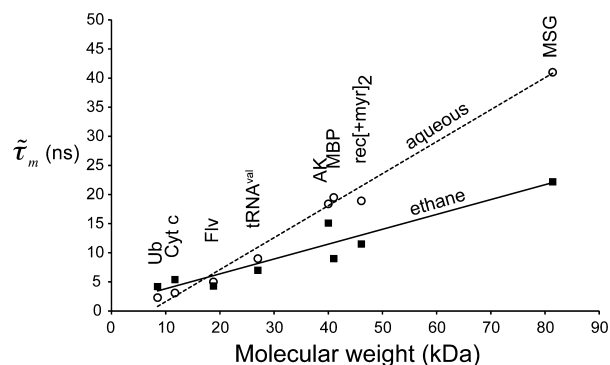


Figure 3. ¹⁵N-TRACT estimates of effective molecular reorientation times (τ_m) of six proteins and tRNA^{val} encapsulated in 10MAG/LDAO reverse micelles in liquid ethane (■) or free in aqueous solution (○). The rec[+myr] point is interpreted as a dimer. All data were recorded at 25 °C. Error bars, as propagated from the quality of the relaxation fits, are smaller than the size of the symbols shown. As addressed in the text, the primary source of error in the TRACT analysis is the inherent assumption of no internal motion.

The optimal sample conditions obtained in pentane were generally transferable to ethane although higher concentrations of the cosurfactant hexanol were often required (see SI for detailed sample conditions). Hexanol significantly lowers the pressure required for forming stable reverse micelle samples, and the resulting reduced pressure lowers the viscosity and therefore reduces the molecular reorientation time.³⁴ After the sample is fully formed inside the mixing chamber it is transferred to a specialized NMR cell.¹⁷ Six of the seven

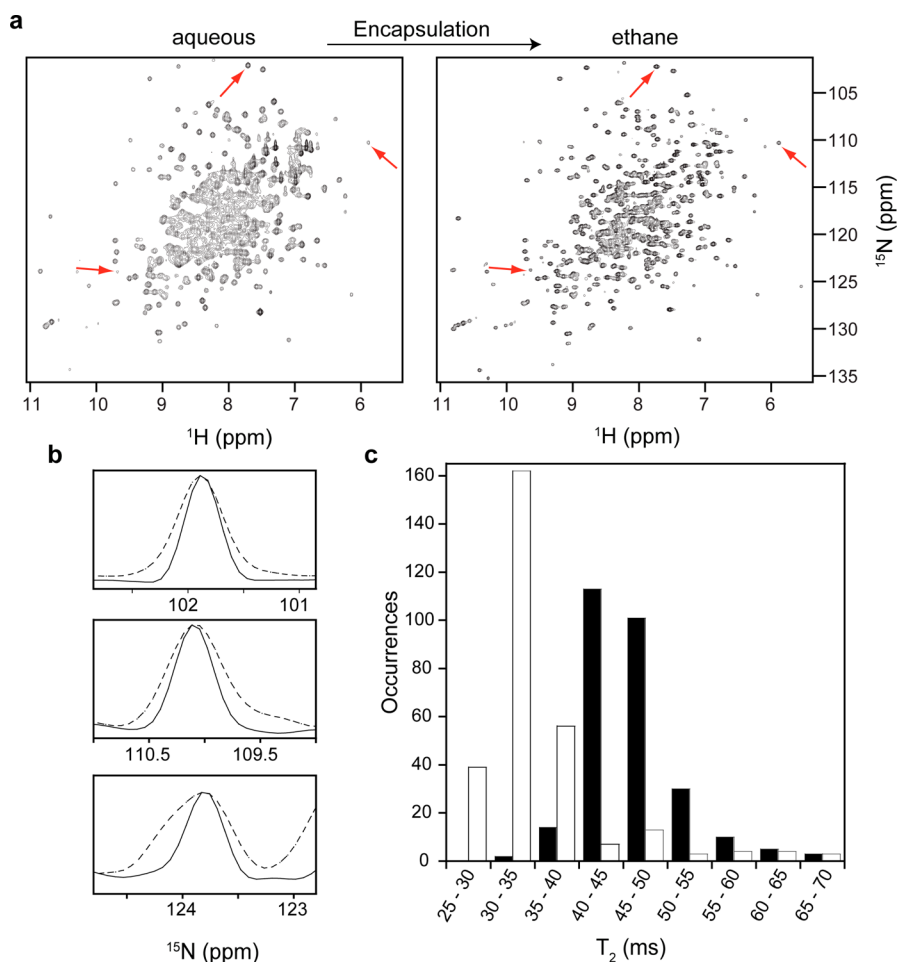


Figure 4. (a) ^{15}N HSQC spectra are shown of MBP in aqueous solution and encapsulated in 10MAG/LDAO reverse micelles dissolved in liquid ethane. Spectra were collected to have comparably high signal-to-noise for direct comparison of line widths. (b) One-dimensional normalized ^{15}N cross sections (aqueous: dashed lines, RM: solid lines) of three cross peaks (red arrows in a) are shown to illustrate the narrowed line widths as a result of improved tumbling upon encapsulation. (c) ^{15}N T_2 values were measured for 278 and 291 sites in the encapsulated (black bars) and aqueous (white bars) MBP samples, respectively, at 750 MHz. A histogram illustrates the overall improvement in relaxation behavior of the encapsulated protein as a result of improved tumbling. The difference in average T_2 values (35 and 46 ms for aqueous and encapsulated protein, respectively) corresponds to a 31% improvement and correlates well the $\sim 32\%$ decrease in rotational correlation time.

soluble proteins were stably encapsulated in ethane. ^{15}N HSQC spectra of these proteins show excellent agreement with aqueous samples (Figures 2c, 4a, 5a, and SI Figure S1). The encapsulation pressures required for preparation in ethane ranged from 275 to 480 bar, which are well below that typically required to significantly perturb the structure and dynamics of folded proteins.³⁵ Long-term stability of the ethane samples at room temperature ranged from more than 4 months for Flv, to 6 weeks for MSG, MBP, Cyt *c*, Ub, and 1 week for AK. The samples of AKR in ethane were not stable for more than a day. Determination of optimal encapsulation conditions in ethane required optimization of hexanol concentration, W_0 , and encapsulation pressure for each of the proteins tested. In general, optimal conditions were identified after only a few (~ 5 or less) tests. Once optimal conditions were identified, these proved to be highly reproducible ($\tilde{\tau}_m \pm 2$ ns). AKR proved unstable in liquid ethane despite numerous tests for optimal conditions. Subsequent to these tests, several other soluble, globular proteins have been tested for encapsulation in 10MAG/LDAO mixtures. To date, only one has been identified that does not encapsulate in 10MAG/LDAO. Encapsulation of

integral membrane proteins in 10MAG/LDAO mixtures has not yet been examined.

The ^{15}N -TRACT experiment,¹⁸ which measures the relaxation rates of the α and β spin states of the amide ^{15}N , was used to estimate the protein's effective molecular reorientation time ($\tilde{\tau}_m$). Although this method systematically underestimates the true molecular reorientation time (τ_m), it provides a rapid method for comparing the tumbling of proteins in reverse micelle and aqueous solutions. The error that results from the rigid body assumption inherent in the TRACT analysis is far greater than the error resulting from the fits to the relaxation profiles. In general, the errors resulting from the quality of the relaxation fits are on the order of the sizes of the symbols shown in Figure 3. Comparing the $\tilde{\tau}_m$ values shows that macromolecules larger than ~ 20 kDa can be made to tumble faster than in aqueous solution when encapsulated and prepared in liquid ethane (Figure 3). For example, encapsulated MBP and MSG showed approximately 50% reduction in $\tilde{\tau}_m$. However, it is important to note that, because the TRACT experiment underestimates the true rotational correlation time, the actual advantage may be more modest. To examine this, the rotational correlation time of

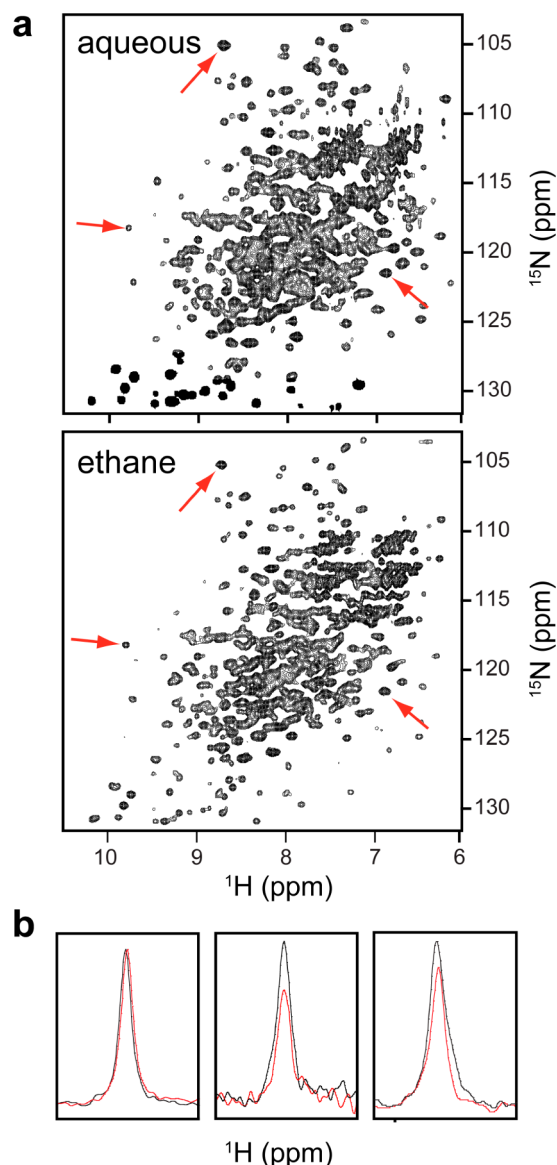


Figure 5. (a) ^{15}N -TROSY spectra are shown of MSG in aqueous solution and encapsulated in 10MAG/LDAO reverse micelles in liquid ethane. These spectra were collected with the same total acquisition time and show comparable signal-to-noise despite the reverse micelle sample containing approximately one-third of the protein as that of the aqueous sample. (b) ^1H cross sections of exemplary (red arrows in a) cross peaks are shown for aqueous (red) and encapsulated (black) MSG.

MBP encapsulated in 75 mM 10MAG/LDAO was determined with a full suite of ^{15}N -relaxation experiments to be 15.5 ns.¹⁹ This corresponds to a markedly slower tumbling behavior than indicated by the TRACT analysis (8.9 ns), but a similar discrepancy was noted previously for the TRACT estimation of tumbling for aqueous MBP.¹⁶

Based on this more rigorous measurement of encapsulated MBP tumbling in ethane, the true improvement in rotational correlation time (15.5 ns for RM versus 23 ns for aqueous solution³⁶) is ~32%.

It should also be noted that some trade-off exists between optimal encapsulation efficiency (i.e., concentration of protein in the final sample) and molecular tumbling. In general, increasing the amount of surfactant in the reverse micelle

system permits encapsulation of higher concentrations of protein, but the tumbling improvement at high surfactant concentrations is slightly reduced and there is the potential for partial alignment of reverse micelle systems at high surfactant concentrations.³⁷

As an example, the optimal sample conditions for MBP in ethane were determined to be at 75 mM total surfactant with 100 mM hexanol. Because AK is more difficult to concentrate in aqueous solution, higher surfactant concentrations (100–150 mM) and higher water loading ($W_0 = 20$ versus 12 for MBP) were required for this protein in order to achieve appropriate encapsulated concentrations (80–100 μM) for efficient collection of NMR data. As shown in Figure 3, the tumbling of MBP in ethane is better than that of AK due to this difference in surfactant conditions. The spectral improvements in tumbling are demonstrated in Figure 4 for MBP encapsulated in ethane as compared to the aqueous protein. The ^{15}N HSQC spectrum of encapsulated MBP shows improved resolution due to narrowing of the resonance lines. This narrowing can more clearly be seen in the one-dimensional spectra given. In addition, the distribution of ^{15}N T_2 values is shifted markedly toward longer relaxation times for the encapsulated protein, demonstrating a general improvement in the relaxation properties of the encapsulated protein. This T_2 advantage not only translates to improved line widths but also provides substantial gains in coherence transfer efficiencies in multidimensional NMR experiments.¹

It is also important to consider that the sensitivity of a modern cryoprobe with RM samples is markedly better than that with aqueous solutions due to the low conductivity of the reverse micelle solution.³⁸ This results in improved signal-to-noise per unit of protein in the encapsulated sample. In combination with the improved tumbling and resultant line narrowing and improved coherence transfer, encapsulation can produce substantially improved signal-to-noise. This is particularly true for larger proteins. For example, the spectra shown in Figure 5 demonstrate that comparable signal-to-noise is obtained for encapsulated MSG as compared to the aqueous condition using the same amount of signal averaging (i.e., identical collection time) but less than half the protein concentration of the aqueous sample. In summary, the successful encapsulation of a diverse set of globular proteins up to 81 kDa in ultralow viscosity ethane shows that 10MAG/LDAO is a general surfactant system for comprehensive reverse micelle NMR.

Concentration by Injection–Evaporation Method. The direct injection method (Figure 1c) is the simplest approach for preparing homogeneous solutions of encapsulated macromolecules. Such solutions are usually prepared under water-limited conditions to obtain the desired water loading (W_0) and fast molecular tumbling. Thus, the concentration of protein in the injected solution defines the final concentration of encapsulated protein. If the protein cannot be sufficiently concentrated, the direct injection method will fail to provide a sufficiently high concentration of encapsulated protein to allow facile multidimensional NMR spectroscopy. For example, using a 1 mM protein stock solution would result in a final concentration of encapsulated protein of only 18 μM with W_0 of 10 and 100 mM surfactant.

To address this limitation, a method was developed that allows fewer soluble macromolecules to be encapsulated by employing successive rounds of injection of a dilute solution followed by evaporation of excess water. We call this procedure

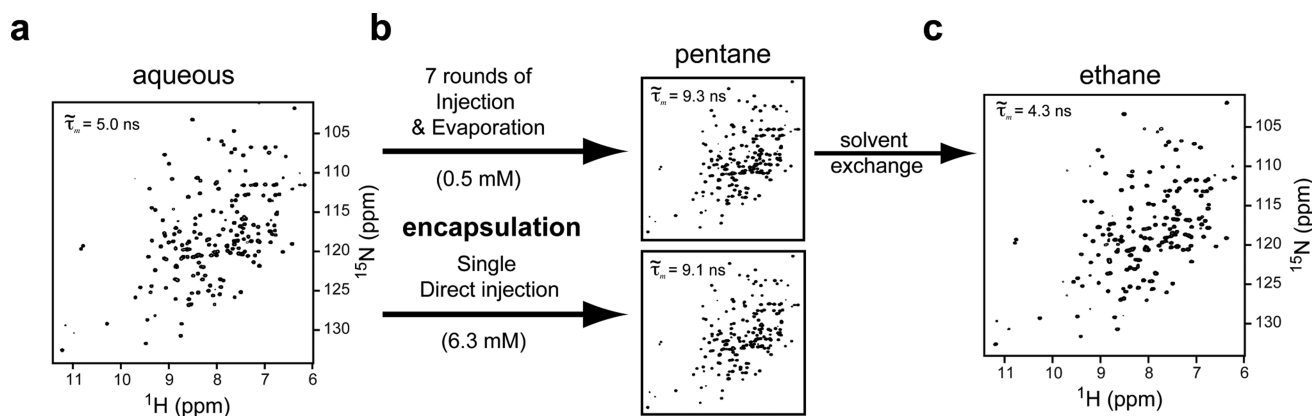


Figure 6. The injection–evaporation method of encapsulation eliminates the requirement for millimolar protein concentrations. (a) Reference ^{15}N HSQC spectrum of $500\ \mu\text{M}$ Flv in aqueous solution. (b) ^{15}N HSQC spectrum of $200\ \mu\text{M}$ encapsulated Flv dissolved in pentane prepared by direct injection using $6.3\ \text{mM}$ Flv (bottom) and prepared by seven rounds of injection–evaporation using a $500\ \mu\text{M}$ Flv stock solution (top). (c) The effective tumbling rate of Flv can be greatly increased by subsequent solvent exchange to ethane. All data were recorded at $25\ ^\circ\text{C}$ and at $500\ \text{MHz}$ (^1H) and processed identically.

the *injection–evaporation* method. The injection–evaporation method is illustrated using a solution of $500\ \mu\text{M}$ flavodoxin and performing seven rounds of protein injection and water evaporation (Figure 6).

The first round of protein injection yielded an encapsulated flavodoxin concentration of $\sim 30\ \mu\text{M}$. After the seventh round the concentration was $200\ \mu\text{M}$. In this example, this allows for a 12-fold reduction in the starting protein concentration ($6.3\ \text{mM}$). The ^{15}N HSQC spectra of encapsulated flavodoxin prepared by injection–evaporation or direct injection were identical (Figure 6b). Furthermore, the flavodoxin sample prepared by the injection–evaporation method could be redissolved in liquid ethane after partial evaporation of the pentane solvent (Figure 6). Thus, the advantages of the injection–evaporation method can be combined with the improved molecular tumbling offered by ultralow viscosity ethane.

10MAG/LDAO as a Membrane Mimetic for Lipid-Modified Proteins. Post-translational lipid modification of proteins, such as attachment of myristate or isoprene groups, is responsible for a variety of specialized functions including localization at membranes or hydrophobic molecular switch-like behavior.³⁹ Exposure of the hydrophobic lipid to water can lead to poor solution behavior that severely compromises structural studies. Consequently, high-resolution structures of lipid-modified proteins in the putative membrane-anchored state obtained using standard NMR spectroscopy or crystallography are surprisingly rare. It was recently shown that myristoylated recoverin and myristoylated HIV matrix protein could be stably encapsulated in CTAB/hexanol reverse micelles in the lipid-extruded state.⁵ However, CTAB is cationic and has electrostatic properties different from those of natural lipid bilayers, and this mismatch may become limiting. In contrast, the 10MAG/LDAO surfactant system more closely resembles the lipids of biological membranes. The zwitterionic LDAO headgroup mimics the phosphatidylcholine headgroup, and 10MAG is a glycerol group esterified to a fatty acid.

The $23\ \text{kDa}$ myristoylated human recoverin (Rec[+myr]), which acts as a Ca^{2+} sensor in the visual system,⁴⁰ was used to test if 10MAG/LDAO could support lipid-anchored proteins. The myristoyl group is extruded upon calcium binding.⁴⁰ Calcium-loaded Rec[+myr] was efficiently encapsulated at $100\ \mu\text{M}$ in 10MAG/LDAO in both pentane and ethane at a water

loading of 12. The ^{15}N HSQC spectra of encapsulated Rec[+myr] were very similar to spectra of natively folded, Ca^{2+} -bound, myristoyl-extruded protein (see refs 5 and 40 and Figure 7). The ^{15}N -TRACT measurements showed much faster

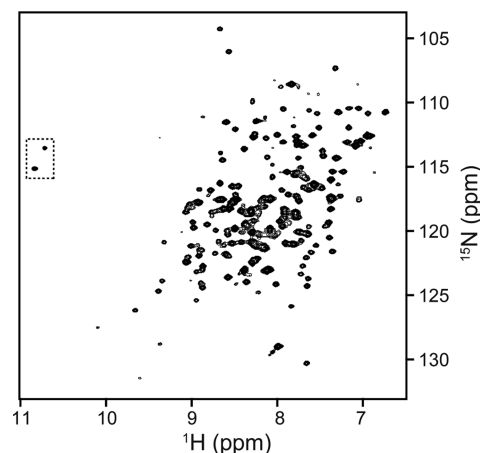


Figure 7. 10MAG/LDAO provides a membrane mimetic environment for NMR spectroscopy of membrane-anchored proteins. ^{15}N HSQC $600\ \text{MHz}$ spectrum of encapsulated calcium-saturated myristoylated recoverin. The dashed line box highlights two cross peaks that are assigned to two Gly residues involved in stabilizing the Ca^{2+} -bound, myristoyl-extruded protein conformation.^{5,40} Sample prepared in ethane at $100\ \mu\text{M}$ Rec[+myr] and $W_0 = 12$ in $100\ \text{mM}$ 10MAG/LDAO at $450\ \text{bar}$.

molecular tumbling in ethane than in pentane ($\tilde{\tau}_m = 11.7$ and $18.8\ \text{ns}$, respectively). Interestingly, the $\tilde{\tau}_m$ values suggested that two Rec[+myr] molecules were encapsulated in occupied reverse micelles. A similar observation was made in the previous study of Rec[+myr] encapsulated in CTAB/hexanol,⁵ suggesting that the protein in the lipid-extruded state is a dimer. The physiological significance of this apparent homodimerization remains to be established.⁴¹

Encapsulation of RNA. DNAs and RNAs represent a significant challenge to solution NMR spectroscopy because they are built from only four different nucleotides and the proton and carbon resonances are highly overlapped due to their narrow chemical shift ranges.^{42–45}

The 27 kDa natively modified valine tRNA (tRNA^{val}) from *E. coli*⁴⁶ was employed here to evaluate the 10MAG/LDAO surfactant system for NMR studies of nucleic acids. The structure and dynamics of tRNA^{val} have been extensively studied,⁴⁷ and it therefore serves as a model system for medium-sized RNAs. ¹⁵N-labeled tRNA^{val} was encapsulated at 100 μM in 10MAG/LDAO reverse micelles in both pentane and ethane using the procedures developed above for proteins. The imino region of the ¹⁵N HSQC spectrum of encapsulated tRNA^{val} is indicative of a natively folded macromolecule using a buffer that included 5 mM Mg²⁺ (Figure 8).

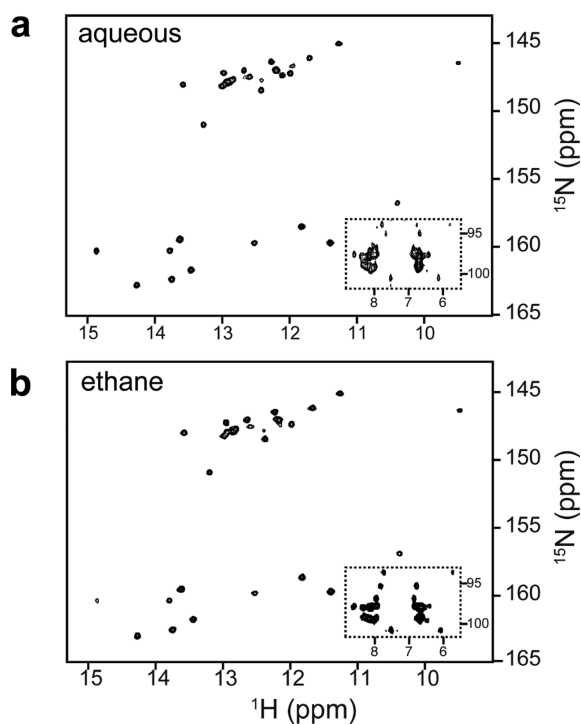


Figure 8. High-fidelity encapsulation of tRNA^{val}. ¹⁵N HSQC spectra of the imino region of tRNA^{val} acquired at 500 MHz (¹H) (a) aqueous solution at 200 μM with 16 scans per FID and (b) encapsulated in 150 mM 10MAG/LDAO and dissolved in ethane at 450 bar at $W_0 = 9$ at 100 μM with 32 scans per FID. The dashed line boxes highlight amino cross peaks, folded in the ¹⁵N chemical shift dimension, showing somewhat improved signal-to-noise for the encapsulated RNA compared to RNA tumbling free in aqueous solution. The tRNA was prepared in 10 mM sodium phosphate (pH 6.8), 80 mM NaCl, 5 mM MgCl₂, 0.1 mM EDTA. Recorded at 25 °C.

Interestingly, amino resonances were sharper and consequently better resolved for the tRNA encapsulated in ethane (at relatively low water loading $W_0 = 9$) than in free solution (boxes in Figure 8). This is partially related to the reduced effective molecular reorientation time ($\tilde{\tau}_m = 7.0$ and 9.0 ns, for the encapsulated and aqueous tRNAs, respectively). In addition, many A, C, and G amino protons are in the intermediate exchange regime in aqueous solution due to either rotation about the C–N bond, which has partial double bond character, or through the effects of hydrogen exchange with water. Hydrogen exchange chemistry is slowed in the reverse micelle,^{10,11,48,49} and the corresponding reduction in hydrogen exchange rates will tend to sharpen the amino hydrogen resonances. Furthermore, the relatively high effective viscosity of the water core of reverse micelles^{48–50} would also tend to

slow conformational exchange processes toward the slow exchange time regime. Conversely, the imino protons are in the slow exchange regime in bulk solution, and their resonances are largely unaffected by the slowed hydrogen exchange chemistry or the increased viscosity of the reverse micelle water core.⁵¹

The effect of slowed hydrogen exchange chemistry on the line shape of exchangeable hydrogens has been observed for encapsulated proteins before, particularly in the ability to resolve NOE cross peaks to hydroxyl hydrogens of serine and threonine residues.^{11,52} These hydroxyl hydrogens exchange far too rapidly in bulk solution for such signals to be observed, but they are visible upon encapsulation. At water loadings less than ~20, the water dynamics and hydrogen exchange rates are considerably slower than in bulk water.^{10,11,48,49} Many RNAs require divalent ions for proper folding and function, with Mg²⁺ generally being the physiologically relevant ion.⁵³ The zwitterionic character of the 10MAG/LDAO surfactant system means that neither the RNA nor the metal ions required for correct folding/function of the macromolecule are likely to interact to any significant extent with the surfactant. Furthermore, since nucleic acids all carry a large number of negative charges, they will have similar overall electrostatic surface charges, and encapsulation conditions that work for one nucleic acid, such as tRNA^{val} studied here, should be readily applicable to other nucleic acids.

CONCLUSIONS

A new binary surfactant system for high-resolution solution NMR studies of encapsulated biological macromolecules dissolved in low viscosity fluids has been developed. The performance of 10MAG/LDAO in reverse micelle NMR has been validated with respect to encapsulation efficiency (yield), fidelity, and molecular tumbling behavior using a set of seven proteins and a tRNA. 10MAG/LDAO therefore represents a single surfactant system that can encapsulate with high structural fidelity a broad range of different target macromolecules with molecular weights at least up to 81 kDa. This simplifies the process of preparing reverse micelle NMR samples, which is often plagued by trial and error searches for optimal encapsulation conditions. It has been found that 10MAG/LDAO may be employed with minimal *a priori* assumptions about the properties of a given target protein or RNA to obtain significant reductions in molecular reorientation times at ambient temperature. This is a significant advantage. Results presented here indicate that proteins in the 40 kDa range are rendered completely accessible to the full battery of triple resonance spectroscopy without the limitations imposed by extensive deuteration or use of the TROSY effect. It should also be noted that the dielectric properties of reverse micelle solutions are more optimal for cryogenic probe technology than standard aqueous samples and can provide a 50–100% gain in sensitivity.³⁸

The ability of 10MAG/LDAO to faithfully encapsulate a range of protein sizes and charge states clearly originates from the favorable physicochemical properties of the two surfactant headgroups—a *nonionic* monoacylated glycerol group in 10MAG and a *zwitterionic* amine-*N*-oxide group in LDAO. The nonionic surfactant content (65 mol % 10MAG) combined with the zwitterionic character of LDAO mixture reduces charge–charge interactions in much the same spirit as the triple surfactant system derived from mixtures of anionic, cationic, and neutral polyether surfactants.¹³ Here, however, the

relatively short contour length of the LDAO and 10MAG minimizes the size of the resulting particle and thereby maximizes the effective tumbling time of the encapsulated macromolecule. The surfactant combination of 10MAG and LDAO also provides a very favorable environment for encapsulating proteins of poor solution properties, such as lipid-modified proteins. It also faithfully encapsulates tRNA. Because all nucleic acids have an overall negative electrostatic surface, it is likely that encapsulation by the 10MAG/LDAO surfactant system will generally not be sensitive to the precise sequence of the RNA (or DNA). Finally, the injection–evaporation method allows for the preparation of reverse micelle samples using relatively dilute protein solutions and represents a significant advantage as it avoids the need for concentrated aqueous solutions of the target macromolecule. In conclusion, 10MAG/LDAO provides many aspects of an optimal surfactant system for solution NMR of encapsulated proteins dissolved in low viscosity fluids. It relieves the experimental problems that exist with the currently employed surfactants AOT, CTAB, and triple surfactant mixtures. We anticipate that the 10MAG/LDAO surfactant system will find broad utility in structural and biophysical studies of encapsulated proteins by high-resolution reverse micelle NMR.

■ ASSOCIATED CONTENT

■ Supporting Information

Details of sample preparation. Description and illustration of screens. This material is available free of charge via the Internet at <http://pubs.acs.org>.

■ AUTHOR INFORMATION

Corresponding Author

wand@mail.med.upenn.edu

Notes

The authors declare the following competing financial interest(s): A.J.W. declares a competing financial interest as Member of Daedalus Innovations, LLC, a manufacturer of high-pressure and reverse micelle NMR apparatus..

■ ACKNOWLEDGMENTS

We thank Li Liang for help in protein preparation. The expression plasmid for AKR was a gift from Professor Trevor Penning (Department of Pharmacology, University of Pennsylvania), and we thank Dr. Yi Jin for advice in AKR purification. This work was supported by NIH Grants GM085120 (A.J.W.) and GM086862 (A.P.) and NSF Grant MCB 115803 (A.J.W.). I.D. and N.V.N. gratefully acknowledge postdoctoral fellowships from the Swiss National Science Foundation and the NIH (GM087099), respectively.

■ REFERENCES

- (1) Rule, G. S.; Hitchens, T. K. *Fundamentals of Protein NMR Spectroscopy*; Springer: Dordrecht, 2006.
- (2) Wand, A. J.; Ehrhardt, M. R.; Flynn, P. F. *Proc. Nat. Acad. Sci. U.S.A.* **1998**, *95*, 15299–15302.
- (3) Van Horn, W. D.; Ogilvie, M. E.; Flynn, P. F. *J. Biomol. NMR* **2008**, *40*, 203–211.
- (4) Kielec, J. M.; Valentine, K. G.; Babu, C. R.; Wand, A. J. *Structure* **2009**, *17*, 345–351.
- (5) Valentine, K. G.; Peterson, R. W.; Saad, J. S.; Summers, M. F.; Xu, X.; Ames, J. B.; Wand, A. J. *Structure* **2010**, *18*, 9–16.
- (6) Peterson, R. W.; Anbalagan, K.; Tommos, C.; Wand, A. J. *J. Am. Chem. Soc.* **2004**, *126*, 9498–9499.
- (7) Workman, H.; Flynn, P. F. *J. Am. Chem. Soc.* **2009**, *131*, 3806–3807.
- (8) Babu, C. R.; Hilser, V. J.; Wand, A. J. *Nat. Struct. Mol. Biol.* **2004**, *11*, 352–357.
- (9) Pometun, M. S.; Peterson, R. W.; Babu, C. R.; Wand, A. J. *J. Am. Chem. Soc.* **2006**, *128*, 10652–10653.
- (10) Nucci, N. V.; Pometun, M. S.; Wand, A. J. *J. Am. Chem. Soc.* **2011**, *133*, 12326–12329.
- (11) Nucci, N. V.; Pometun, M. S.; Wand, A. J. *Nat. Struct. Mol. Biol.* **2011**, *18*, 245–249.
- (12) Simorellis, A. K.; Flynn, P. F. *J. Am. Chem. Soc.* **2006**, *128*, 9580–9581.
- (13) Peterson, R. W.; Pometun, M. S.; Shi, Z. S.; Wand, A. J. *Protein Sci.* **2005**, *14*, 2919–2921.
- (14) Doussin, S.; Birlirakis, N.; Georgin, D.; Taran, F.; Berthault, P. *Chemistry* **2006**, *12*, 4170–4175.
- (15) Lefebvre, B. G.; Liu, W.; Peterson, R. W.; Valentine, K. G.; Wand, A. J. *J. Magn. Reson.* **2005**, *175*, 158–162.
- (16) Nucci, N. V.; Marques, B. S.; Bédard, S.; Dogan, J.; Gledhill, J. M., Jr.; Moorman, V. R.; Peterson, R. W.; Valentine, K. G.; Wand, A. L.; Wand, A. J. *J. Biomol. NMR* **2011**, *50*, 421–430.
- (17) Peterson, R. W.; Wand, A. J. *Rev. Sci. Instrum.* **2005**, *76*, No. 094101.
- (18) Lee, D.; Hilty, C.; Wider, G.; Wüthrich, K. *J. Magn. Reson.* **2006**, *178*, 72–76.
- (19) Farrow, N. A.; Muhandiram, R.; Singer, A. U.; Pascal, S. M.; Kay, C. M.; Gish, G.; Shoelson, S. E.; Pawson, T.; Forman-Kay, J. D.; Kay, L. E. *Biochemistry* **1994**, *33*, 5984–6003.
- (20) Lakomek, N. A.; Ying, J.; Bax, A. *J. Biomol. NMR* **2012**, *53*, 209–221.
- (21) Kasinath, V.; Valentine, K. G.; Wand, A. J. *J. Am. Chem. Soc.* **2013**, *135*, 9560–9563.
- (22) Gledhill, J. M., Jr.; Wand, A. J. *J. Biomol. NMR* **2012**, *52*, 79–89.
- (23) Liu, W.; Flynn, P. F.; Fuentes, E. J.; Kranz, J. K.; McCormick, M.; Wand, A. J. *Biochemistry* **2001**, *40*, 14744–14753.
- (24) Liu, W.; Rumbley, J.; Englander, S. W.; Wand, A. J. *Protein Sci.* **2003**, *12*, 2104–2108.
- (25) Liu, W.; Rumbley, J. N.; Englander, S. W.; Wand, A. J. *Protein Sci.* **2009**, *18*, 670–674.
- (26) Luisi, P. L.; Giomini, M.; Pileni, M. P.; Robinson, B. H. *Biochim. Biophys. Acta* **1988**, *947*, 209–246.
- (27) Marques, B. S.; Nucci, N. V.; Dodevski, I.; Wang, W. C.; Athanasoula, E. A.; Jorge, C.; Wand, A. J. *J. Phys. Chem. B* **2013**, DOI: [jp4103349](https://doi.org/10.1021/jp4103349).
- (28) Peterson, R. W.; Lefebvre, B. G.; Wand, A. J. *J. Am. Chem. Soc.* **2005**, *127*, 10176–10177.
- (29) Babu, C. R.; Flynn, P. F.; Wand, A. J. *J. Biomol. NMR* **2003**, *25*, 313–323.
- (30) Ehrhardt, M. R.; Flynn, P. F.; Wand, A. J. *J. Biomol. NMR* **1999**, *14*, 75–78.
- (31) Flynn, P. F.; Milton, M. J.; Babu, C. R.; Wand, A. J. *J. Biomol. NMR* **2002**, *23*, 311–316.
- (32) Gaemers, S.; Elsevier, C. J.; Bax, A. *Chem. Phys. Lett.* **1999**, *301*, 138–144.
- (33) Meier, M.; Fink, A.; Brunner, E. *J. Phys. Chem. B* **2005**, *109*, 3494–3498.
- (34) Peterson, R. W.; Nucci, N. V.; Wand, A. J. *J. Magn. Reson.* **2011**, *212*, 229–233.
- (35) Akasaka, K. *Chem. Rev.* **2006**, *106*, 1814–1835.
- (36) Yang, D.; Kay, L. E. *J. Biomol. NMR* **1999**, *13*, 3–10.
- (37) Valentine, K. G.; Pometun, M. S.; Kielec, J. M.; Baigelman, R. E.; Staub, J. K.; Owens, K. L.; Wand, A. J. *J. Am. Chem. Soc.* **2006**, *128*, 15930–15931.
- (38) Flynn, P. F.; Mattiello, D. L.; Hill, H. D. W.; Wand, A. J. *J. Am. Chem. Soc.* **2000**, *122*, 4823–4824.
- (39) Resh, M. D. *Trends Mol. Med.* **2012**, *18*, 206–214.
- (40) Ames, J. B.; Ishima, R.; Tanaka, T.; Gordon, J. I.; Stryer, L.; Ikura, M. *Nature* **1997**, *389*, 198–202.

- (41) Myers, W. K.; Xu, X.; Li, C.; Lagerstedt, J. O.; Budamagunta, M. S.; Voss, J. C.; Britt, R. D.; Ames, J. B. *Biochemistry* **2013**, *52*, 5800–5808.
- (42) Al-Hashimi, H. M.; Walter, N. G. *Curr. Opin. Struct. Biol.* **2008**, *18*, 321–329.
- (43) Dominguez, C.; Schubert, M.; Duss, O.; Ravindranathan, S.; Allain, F. H. *Prog. Nucl. Magn. Reson. Spectrosc.* **2011**, *58*, 1–61.
- (44) Latham, M. P.; Brown, D. J.; McCallum, S. A.; Pardi, A. *ChemBioChem* **2005**, *6*, 1492–1505.
- (45) Lu, K.; Miyazaki, Y.; Summers, M. F. *J. Biomol. NMR* **2010**, *46*, 113–125.
- (46) Yue, D. X.; Kintanar, A.; Horowitz, J. *Biochemistry* **1994**, *33*, 8905–8911.
- (47) Vermeulen, A.; McCallum, S. A.; Pardi, A. *Biochemistry* **2005**, *44*, 6024–6033.
- (48) Park, S.; Moilanen, D. E.; Fayer, M. D. *J. Phys. Chem. B* **2008**, *112*, 5279–5290.
- (49) Fenn, E. E.; Wong, D. B.; Fayer, M. D. *Proc. Nat. Acad. Sci U.S.A.* **2009**, *106*, 15243–15248.
- (50) Pieniazek, P. A.; Lin, Y. S.; Chowdhary, J.; Ladanyi, B. M.; Skinner, J. L. *J. Phys. Chem. B* **2009**, *113*, 15017–15028.
- (51) Lee, Y.-M.; Lee, E.-H.; Seo, Y.-J.; Kang, Y.-M.; Ha, J.-H.; Kim, H.-E.; Lee, J.-H. *Bull. Korean Chem. Soc.* **2009**, *30*, 2197–2198.
- (52) Babu, C. R.; Flynn, P. F.; Wand, A. J. *J. Am. Chem. Soc.* **2001**, *123*, 2691–2692.
- (53) Feig, A. L.; Uhlenbeck, O. C. In *The RNA World*; Gesteland, R. F., Cech, T. R., Atkins, J. F., Eds.; Cold Spring Harbor Laboratory: Plainview, NY, 1999, pp 287–319.